

Bipartite entanglement induced by classically-constrained quantum dissipative dynamics

Adrián A. Budini

*Consejo Nacional de Investigaciones Científicas y Técnicas,
Centro Atómico Bariloche, Avenida E. Bustillo Km 9.5, (8400) Bariloche, Argentina*

(Dated: January 25, 2022)

The properties of some complex many body systems can be modeled by introducing in the dissipative dynamics of each single component a set of kinetic constraints that depend on the state of the neighbor systems. Here, we characterize this kind of dynamics for two quantum systems whose independent dissipative evolutions are defined by a Lindblad equation. The constraints are introduced through a set of projectors that restrict the action of each single dissipative Lindblad channel to the state of the other system. Conditions that guaranty a classical interpretation of the kinetic constraints are found. The generation and evolution of entanglement is studied for two optical qubits systems. Classically constrained dissipation leads to a stationary state whose degree of entanglement depends on the initial state. Nevertheless, independently of the initial conditions, a maximal entangled state is generated when both systems are subjected to the action of local Hamiltonian fields that do not commute with the constraints. The underlying physical mechanism is analyzed in detail.

PACS numbers: 03.65.Yz, 03.67.Mn

Keywords: open quantum systems, decoherence, entanglement characterization

I. INTRODUCTION

Superposition of different states corresponding to a bipartite quantum system may lead to entanglement, that is, quantum states whose statistical properties can not be reproduced with local stochastic variables. Due to its central role in quantum information and quantum computation [1], in the last years and ever-increasing interest has been paid to its characterization [2].

Superposition of bipartite quantum states are degraded by interaction with uncontrollable degrees of freedom [3]. In contrast to quantum decoherence, the decay of entanglement, measured for example by concurrence [4], has non-usual properties such as its finite time decay [5] as well as the possibility of its sudden appearance at posterior times [6]. Non-standard decay properties were also found in the classical [7] and quantum [8] contributions of the total correlation (mutual information) between two systems [9, 10].

Even when the environment destroy the nonlocal properties of entanglement, it may also play a constructive role. The creation of entanglement by the action of a common bath was studied in many different physical situations [11–25]. Special interest have been paid to optical systems such as the Dicke model [21–23] where the dissipative decay dynamics is induced by interaction with the background electromagnetic field.

Added to the individual irreversible dynamics, dissipation of systems embedded in complex many body arrangements may involves extra elements. For example, in quantum aggregates [26] the effects of a bath on a subsystem can be dependent on the state of another site [27]. This kind of constrained dissipation also arises in glassy systems. In fact, in contrast to static disordered interactions, glassiness can also be induced by dynamical con-

straints [28–32]. In a classical context, this situation is usually modeled by a Markovian master equation where the transition rates of each system depend on the state of the neighbors systems [32]. In Ref. [33] it was introduced a quantum version where the underlying evolution is given by a Lindblad equation and a set of projection operators introduce the constraints.

Constrained dissipation lead to an effective interaction between subsystems. As the dissipative dynamics admits a Markovian description [32, 33], we expect that some entanglement may be generated by this mechanism [11]. Motivated by the previous physical situations, in this paper we study the production and evolution of entanglement for systems whose dissipative evolution is a constrained one. Our main theoretical goal is to characterize which kind of stationary entangled states may be generated by the constraints when they admit a classical interpretation [32]. The classicality property seems to be a very restrictive condition for the generation of entanglement. Nevertheless, focusing our analysis on a bipartite dynamics, we find that the joint action of classical dissipative constraints and local unitary evolutions may drive the dynamics to maximal entangled states.

We introduce a generalized definition of constrained dissipation, where the dynamical action of each system's dissipative channel can only happens when the other system is in a given quantum state [33]. Conditions that guarantee the “classicality” of the kinetic constraints is provided. In such a case, the system's reduced evolutions are defined by a Lindblad rate equation [34, 35]. The entanglement generation is analyzed for two optical-like qubits systems whose individual decay dynamics can only happens when the other system is in the lower state. The entanglement is characterized both in the transitory and stationary regimes. In order to provide an deeper char-

acterization of the dynamics, added to the entanglement behavior, we also study its relation with the quantum and classical correlations build up between both systems [36–40].

The paper is organized as follows. In Sect. II we provide a generalized definition of constrained dissipation for bipartite dynamics. Conditions that guarantee the classicality of the kinetic constraints is provided. In Sec. III we analyze the entanglement evolution for two optical-like qubits. In Sec. IV, the interplay between the constraints and local external fields that lead to a maximal entangled state is investigated. In Sec. V we provide the Conclusions. In the appendix we briefly review the utilized entanglement measure as well as the definitions of quantum and classical correlations.

II. CONSTRAINED DISSIPATION

We consider two systems A and B , both of them coupled to independent Markovian reservoirs. The dissipative Lindblad evolution [3] induced by each bath is denoted by $\mathcal{L}_A[\rho]$ and $\mathcal{L}_B[\rho]$. The bipartite density matrix describing both systems is $\rho_{AB}(t)$. In order to focus on the dissipative structure, we assume that both Lindblad superoperators commute with their respective system unitary evolutions. Hence, in an interaction representation, the evolution of $\rho_{AB}(t)$ can be written as

$$\frac{d\rho_{AB}(t)}{dt} = \mathcal{L}_A[\rho_{AB}(t)] + \mathcal{L}_B[\rho_{AB}(t)]. \quad (1)$$

Each contribution is defined by the expressions

$$\mathcal{L}_A[\rho] = \frac{1}{2} \sum_i \gamma_A^i ([A_i, \rho A_i^\dagger] + [A_i \rho, A_i^\dagger]), \quad (2a)$$

$$\mathcal{L}_B[\rho] = \frac{1}{2} \sum_i \gamma_B^i ([B_i, \rho B_i^\dagger] + [B_i \rho, B_i^\dagger]), \quad (2b)$$

where $\{\gamma_A^i, \gamma_B^i\}$ are the dissipative rates of each dissipative channel defined by the operators $\{A_i, B_i\}$. In each sum, the index run from one up to the dimension of the system Hilbert space. For simplifying the notation, from now on we assume $\dim(\mathcal{H}_A) = \dim(\mathcal{H}_B)$.

The operators $\{A_i\}$ and $\{B_i\}$ only act, respectively, on the Hilbert space of system A and B . Hence, the bipartite evolution Eq. (1) is defined under the association

$$A_i \rightarrow A_i \otimes I_B, \quad B_i \rightarrow I_A \otimes B_i. \quad (3)$$

The identity operators (I_A, I_B) indicates the absence of any correlation between the dynamics induced by each bath.

Constrained dissipation means that the action of each dissipative channel (operators A_i and B_i) only happen when the other system (B and A) is in a given subspace or quantum state. These kinetic constraints are introduced through the replacements

$$A_i \rightarrow A_i \otimes \mathcal{Q}_i, \quad B_i \rightarrow \mathcal{P}_i \otimes B_i, \quad (4)$$

where $\{\mathcal{P}_i\}$ and $\{\mathcal{Q}_i\}$ are orthogonal projectors operators, $\mathcal{P}_i \mathcal{P}_j = \delta_{ij} \mathcal{P}_i$, $\mathcal{Q}_i \mathcal{Q}_j = \delta_{ij} \mathcal{Q}_i$, acting on systems A and B respectively. With these definitions it become evident that the action of a given reservoir over its system is dynamically restricted or conditioned by the state of the other system. Notice that in contrast with the approach of Ref. [33], here each Lindblad channel may be characterized by a different projector. Trivially, the present generalization recover that case by taking $\mathcal{P}_i \rightarrow \mathcal{P}$, and $\mathcal{Q}_i \rightarrow \mathcal{Q}$.

Some general characterization of the constrained dissipation induced by the operators (4) can be achieved after assuming some properties for the set of projectors operators.

A. Stationary properties

We assume that the un-constrained evolution, Eqs. (2) and (3), has a unique and separable stationary state

$$\rho_{AB}^\infty = \lim_{t \rightarrow \infty} \rho_{AB}(t) = \rho_A^\infty \otimes \rho_B^\infty. \quad (5)$$

Hence, we may ask about the effects of the constraints (4) on this state. While a general answer is not possible, under the conditions

$$[\mathcal{P}_i, \rho_A^\infty] = [\mathcal{Q}_i, \rho_B^\infty] = 0, \quad (6)$$

it is simple to realize that the stationary state remains the same. Nevertheless, it is not possible to guarantee that any initial condition relax to the same stationary state. In general, only a subset of initial conditions $\rho_{AB}(0) \in \{\mathcal{H}_0\}$ fulfill this condition,

$$\rho_{AB}^\infty|_{\{\mathcal{H}_0\}} = \lim_{t \rightarrow \infty} \rho_{AB}(t)|_{\{\mathcal{H}_0\}} = \rho_A^\infty \otimes \rho_B^\infty, \quad (7)$$

where $\mathcal{H}_0 \in \mathcal{H}_{AB}$ is a subspace over the set of all possible initial conditions for A and B . This property arises because the dynamic becomes reducible, that is, the Hilbert space decompose into different subsets between which no transition is possible. Free decoherence subspaces as well as dark states may characterize the subspace complementary to \mathcal{H}_0 . These features are explicitly shown in the next sections.

B. Classical constraints

Given the quantum nature of both systems, the constraints can only be understood when acting in Hilbert space. Here, we found which conditions permit us to read the kinetic constraints in a classical way [32].

Let assume the completeness properties

$$\sum_i \mathcal{P}_i = I_A, \quad \sum_i \mathcal{Q}_i = I_B. \quad (8)$$

Therefore, the partial matrixes $\rho_A(t) = \text{Tr}_B[\rho_{AB}(t)]$ and $\rho_B(t) = \text{Tr}_A[\rho_{AB}(t)]$ can be written as

$$\rho_A(t) = \sum_i \text{Tr}_B[\mathcal{Q}_i \rho_{AB}(t)] \equiv \sum_i \rho_A^{(i)}(t), \quad (9a)$$

$$\rho_B(t) = \sum_i \text{Tr}_A[\mathcal{P}_i \rho_{AB}(t)] \equiv \sum_i \rho_B^{(i)}(t). \quad (9b)$$

The matrix $\rho_A^{(i)}(t)$ [$\rho_B^{(i)}(t)$] can be read as the conditional evolution of system A (B) given that system B (A) is in the state defined by the projector \mathcal{Q}_i (\mathcal{P}_i). In general, the evolution of these conditional states can not be written in a closed way without involving other matrix elements (coherences) contained in $\rho_{AB}(t)$. A classical interpretation of the constraints can only be achieved when these last objects does not participate in the dynamics of the auxiliary states. That is, it should be possible to write a closed evolution for the set $\{\rho_A^{(i)}(t)\}$ as well as for the set $\{\rho_B^{(i)}(t)\}$.

From Eqs. (2) and (4), it is simple to realize that the previous classicality condition is satisfied when the projectors are closed under the transitions induced by each dissipative channel,

$$A_j^\dagger \mathcal{P}_i A_j = \sum_k \alpha_{ik}^j \mathcal{P}_k, \quad B_j^\dagger \mathcal{Q}_i B_j = \sum_k \beta_{ik}^j \mathcal{Q}_k. \quad (10)$$

Here, α_{ik}^j and β_{ik}^j are real positive coefficients that also satisfy $\alpha_{ii}^j = \beta_{ii}^j = 0$. These relations, jointly with Eq. (8), implies that $A_j^\dagger A_j = \sum_{i,k} \alpha_{ik}^j \mathcal{P}_k$, and $B_j^\dagger B_j = \sum_{i,k} \beta_{ik}^j \mathcal{Q}_k$. By introducing the closure condition (10) in the constrained evolution, Eqs. (1) and (4), we get $[\rho_A^{(i)}(t) \rightarrow \rho_A^{(i)}]$

$$\begin{aligned} \frac{d\rho_A^{(i)}}{dt} &= \gamma_A^i \left(A_i \rho_A^{(i)} A_i^\dagger - \frac{1}{2} \{A_i^\dagger A_i, \rho_A^{(i)}\}_+ \right) \\ &+ \sum_{j,k} b_{ij}^k \mathcal{P}_k \rho_A^{(j)} \mathcal{P}_k - \frac{1}{2} \sum_{j,k} b_{ji}^k \{ \mathcal{P}_k, \rho_A^{(i)} \}_+, \end{aligned} \quad (11a)$$

jointly with the symmetrical expression $[\rho_B^{(i)}(t) \rightarrow \rho_B^{(i)}]$

$$\begin{aligned} \frac{d\rho_B^{(i)}}{dt} &= \gamma_B^i \left(B_i \rho_B^{(i)} B_i^\dagger - \frac{1}{2} \{B_i^\dagger B_i, \rho_B^{(i)}\}_+ \right) \\ &+ \sum_{j,k} a_{ij}^k \mathcal{Q}_k \rho_B^{(j)} \mathcal{Q}_k - \frac{1}{2} \sum_{j,k} a_{ji}^k \{ \mathcal{Q}_k, \rho_B^{(i)} \}_+. \end{aligned} \quad (11b)$$

With $\{\dots\}_+$ we denote an anticommutation operation. Furthermore, the rate coefficients read

$$a_{ij}^k = \gamma_A^k \alpha_{ij}^k, \quad b_{ij}^k = \gamma_B^k \beta_{ij}^k. \quad (12)$$

Equations (11a) and (11b) demonstrate that under the conditions (10) the time evolution of the reduced dynamic of each system can be written in a closed way without involving in an explicit way matrix elements of the

other system. These dynamical equations are a particular case of Lindblad rate equations [34], which describe the more general evolution of a quantum system coupled to a set of classical degrees of freedom [35]. Here, the underlying classical feature of these evolutions can explicitly be shown by introducing the expectation values

$$p_j^i(t) \equiv \text{Tr}_A[\rho_A^{(i)}(t) \mathcal{P}_j], \quad q_j^i(t) \equiv \text{Tr}_B[\rho_B^{(i)}(t) \mathcal{Q}_j]. \quad (13)$$

By using the completeness conditions (8) and the definitions (9) it follow the normalizations $\sum_{ij} p_j^i(t) = 1$ and $\sum_{ij} q_j^i(t) = 1$. Furthermore, Eq. (9) implies the relation $q_j^i(t) = p_j^i(t)$. From the Lindblad rate equations (11) we get the *classical rate equation* $[p_j^i(t) \rightarrow p_j^i]$

$$\frac{dp_j^i}{dt} = \sum_k (a_{jk}^i p_k^i - a_{kj}^i p_j^i) + \sum_k (b_{ik}^j p_j^k - b_{ki}^j p_j^i). \quad (14)$$

The evolution of p_j^i (q_j^i) consists of two contributions. The first one is induced by the diagonal contributions of Eq. (11a) [Eq.(11b)] leading to the classical transitions $k \rightarrow j$ with rates a_{jk}^i (b_{jk}^i). These contributions take into account the fluctuation of system A (B) induced by its own reservoir. The second contribution follows from the nondiagonal term of Eq. (11a) [Eq.(11b)], being defined by the rates b_{ik}^j (a_{ik}^j), corresponding to the transitions $k \rightarrow i$. These terms take into account the fluctuations of the constraints of system A (B) induced by the dissipative dynamics of system B (A).

We conclude that the quantum dynamical constraints Eq. (4) are classical if their influence can read from a (transition) rate evolution, here defined by Eq. (14). In the next section, we study the generation and evolution of entanglement for two qubits characterized by this kind of classically constrained dissipation.

III. CLASSICAL CONSTRAINED DISSIPATION IN TWO QUBITS SYSTEMS

We consider to qubit systems A and B . The state of each one is represented in the basis $|\pm\rangle$. Their density matrix $\rho_{AB}(t)$ evolve as

$$\frac{d\rho_{AB}(t)}{dt} = \frac{-i}{\hbar} [H, \rho_{AB}(t)] + \mathcal{L}[\rho_{AB}(t)]. \quad (15)$$

In the basis $|\pm\rangle$, and in absence of any external field, the unitary contribution is defined by the Hamiltonian

$$H = \frac{\hbar\omega_A}{2} \sigma_z \otimes \mathbf{I}_B + \frac{\hbar\omega_B}{2} \mathbf{I}_A \otimes \sigma_z, \quad (16)$$

where σ_z is the z-Pauli matrix and ω_s ($s = A, B$) are the transition frequencies. A unique dissipative channel define the Lindblad contribution of each system. Hence, $\mathcal{L}[\rho]$ is written as

$$\mathcal{L}[\rho] = \frac{1}{2} \sum_{s=A,B} \gamma_s ([V_s, \rho V_s^\dagger] + [V_s \rho, V_s^\dagger]), \quad (17)$$

where γ_s is the dissipative rate of each system. The operators $\{V_s\}$ characterize the interaction of each system with the environment. For optical arranges, they must be taken as [3]

$$V_A = \sigma \otimes I_B, \quad V_B = I_A \otimes \sigma, \quad (18)$$

where $\sigma = |- \rangle \langle + |$ is the lowering operator. In this case, independently of the initial condition, the stationary state is

$$\rho_{AB}^\infty = \lim_{t \rightarrow \infty} \rho_{AB}(t) = |-- \rangle \langle -- |, \quad (19)$$

that is, independently of the initial conditions, both systems end in the lower state.

A. Classical constraints

The dynamical constraints are written as

$$V_A = \sigma \otimes \mathcal{P}_B, \quad V_B = \mathcal{P}_A \otimes \sigma. \quad (20)$$

We consider the symmetric projectors case

$$\mathcal{P}_A = |- \rangle \langle - |, \quad \mathcal{P}_B = |- \rangle \langle - |. \quad (21)$$

With these constraints, the decay dynamics ($|+\rangle \rightsquigarrow |- \rangle$) of each system is only possible when the other system is in the lower state. We remark that these operators and projectors can be read as a two qubit version of the Fredrickson-Andersen model (with periodic boundary conditions) or East model of Ref. [33] [see Eqs. (4) and (5) of that paper]. Nevertheless, due to the optical motivation, here the effective temperature is zero. Furthermore, the projectors, instead of the upper state, here are defined by the lower state. In spite of the states (lower or upper), the classicality condition (10) is satisfied by Eqs. (20) and (21). A quantum constraint should to violates condition (10), such as for example taking both projectors as $\mathcal{P} = |x_\pm \rangle \langle x_\pm |$, where $|x_\pm \rangle = (1/\sqrt{2})(|+\rangle \pm |- \rangle)$ are the eigenstates of the x -Pauli matrix. In this case, all results of section II do no apply.

Given that the classicality condition (10) is satisfied by Eqs. (20) and (21), the evolution of the partial projected matrixes must be given by a Lindblad rate equation. The partial matrixes $\rho_A(t) = \text{Tr}_B[\rho_{AB}(t)]$ and $\rho_B(t) = \text{Tr}_A[\rho_{AB}(t)]$ can be written as

$$\rho_A(t) = \rho_A^-(t) + \rho_A^+(t), \quad \rho_B(t) = \rho_B^-(t) + \rho_B^+(t), \quad (22)$$

where $\rho_A^-(t) = \text{Tr}_B[\mathcal{P}_B \rho_{AB}(t)]$, $\rho_A^+(t) = \text{Tr}_B[(I_B - \mathcal{P}_B) \rho_{AB}(t)]$, $\rho_B^-(t) = \text{Tr}_A[\mathcal{P}_A \rho_{AB}(t)]$, and $\rho_B^+(t) = \text{Tr}_A[(I_A - \mathcal{P}_A) \rho_{AB}(t)]$. From Eqs. (17) and (20), in an interaction representation with respect to the Hamiltonian (16), we consistently get

$$\frac{d\rho_A^-(t)}{dt} = \gamma_A L[\rho_A^-(t)] + \gamma_B \mathcal{P}_A \rho_A^+(t) \mathcal{P}_A, \quad (23a)$$

$$\frac{d\rho_A^+(t)}{dt} = -\frac{1}{2} \gamma_B \{\mathcal{P}_A, \rho_A^+(t)\}_+, \quad (23b)$$

where $L[\rho] \equiv (1/2)([\sigma, \rho \sigma^\dagger] + [\sigma \rho, \sigma^\dagger])$. Symmetrically,

$$\frac{d\rho_B^-(t)}{dt} = \gamma_B L[\rho_B^-(t)] + \gamma_A \mathcal{P}_B \rho_B^+(t) \mathcal{P}_B, \quad (23c)$$

$$\frac{d\rho_B^+(t)}{dt} = -\frac{1}{2} \gamma_A \{\mathcal{P}_B, \rho_B^+(t)\}_+. \quad (23d)$$

Given the bipartite initial condition $\rho_{AB}(0)$, these equations completely define the reduced dynamics of each system. Correlations between them can only be characterized from the bipartite Lindblad equation (15).

By denoting the product basis as

$$|1\rangle = |++\rangle, \quad |3\rangle = |+-\rangle, \quad (24a)$$

$$|2\rangle = |+-\rangle, \quad |4\rangle = |--\rangle. \quad (24b)$$

the dissipative evolution [Eqs. (17) and (20)] reads

$$\mathcal{L}[\rho] = - \begin{pmatrix} 0 & \frac{\gamma_A}{2} \rho_{12} & \frac{\gamma_B}{2} \rho_{13} & 0 \\ \frac{\gamma_A}{2} \rho_{21} & \gamma_A \rho_{22} & \gamma \rho_{23} & \frac{\gamma_A}{2} \rho_{24} \\ \frac{\gamma_B}{2} \rho_{31} & \gamma \rho_{32} & \gamma_B \rho_{33} & \frac{\gamma_B}{2} \rho_{34} \\ 0 & \frac{\gamma_A}{2} \rho_{42} & \frac{\gamma_B}{2} \rho_{43} & -(\gamma_A \rho_{22} + \gamma_B \rho_{33}) \end{pmatrix}, \quad (25)$$

where $\rho_{ij} = \langle i | \rho | j \rangle$, $i, j = 1, 2, 3, 4$, and $\gamma \equiv (\gamma_A + \gamma_B)/2$. The influence of the constraints can be easily understood by analyzing the diagonal elements of this equation, which in turn define the classical evolution Eq. (14). Evidently, the dynamics take place if at least one of the systems is in the lower state. Therefore, the pure state $|++\rangle \langle ++|$ does not decay at all and is preserved by the evolution. Equivalently, it is a dark state. On the other hand, in the complementary (Hilbert) space, the dynamic is attracted toward the stationary state in absence of constraints, that is, $|-- \rangle \langle -- |$. In fact, condition (6) is also satisfied in this case.

B. Entanglement of the stationary state

Given that the dissipative and unitary generators commute, the stationary state corresponding to the Lindblad evolution (15) can straightforwardly be obtained from Eq. (25). For arbitrary initial conditions, we get

$$\rho_{AB}^\infty = \lim_{t \rightarrow \infty} \rho_{AB}(t) = \begin{pmatrix} p & 0 & 0 & c \\ 0 & 0 & 0 & 0 \\ 0 & 0 & 0 & 0 \\ c^* & 0 & 0 & 1-p \end{pmatrix}, \quad (26)$$

where the matrix elements reads

$$p = \langle ++ | \rho_{AB}(0) | ++ \rangle, \quad (27a)$$

$$c = \langle ++ | \rho_{AB}(0) | -- \rangle. \quad (27b)$$

The stationary partial matrixes are $\rho_A^\infty = \rho_B^\infty = \text{diag}\{p, 1-p\}$ which in agreement with Eqs. (23), imply $\rho_A^-(\infty) = \rho_B^-(\infty) = (1-p) |- \rangle \langle - |$ and $\rho_A^+(\infty) = \rho_B^+(\infty) = p | + \rangle \langle + |$.

The stationary state ρ_{AB}^∞ depends on the initial conditions only when the dark state $|++\rangle$ is populated at the

initial time. In this situation, some entanglement may be found in the long-time limit. Even more, from Eq. (26) we deduce that two Bell states are preserved by the dynamics. That is, for $|\Phi_{\pm}\rangle$ at any time (in an interaction representation) the density matrix satisfies

$$\rho_{AB}(t) = \rho_{AB}(0) = |\Phi_{\pm}\rangle \langle \Phi_{\pm}|. \quad (28)$$

As usual, the Bell basis is denoted as $|\Phi_{\pm}\rangle \equiv \frac{1}{\sqrt{2}}(\pm|++\rangle + |--\rangle)$, and $|\Psi_{\pm}\rangle \equiv \frac{1}{\sqrt{2}}(\pm|+-\rangle + |-+\rangle)$.

Evidently, the states (28) are preserved because they are a superposition of the dark state and the stationary state corresponding to the complementary Hilbert space. In general, the stationary state is not a maximal entangled one. Its degree of entanglement can be measured by concurrence $C[\rho_{AB}^{\infty}]$ [4]. In Appendix we get

$$C[\rho_{AB}^{\infty}] = 2|c|. \quad (29)$$

The capacity of the dissipative dynamics for “generating” entanglement can be characterized by maximizing the concurrence $C[\rho_{AB}^{\infty}]$ given that the systems begin in an arbitrary separable state. Therefore, we take

$$\rho_{AB}(0) = \rho_{\mathbf{n}_a} \otimes \rho_{\mathbf{n}_b}, \quad (30)$$

where each matrix is defined from

$$\rho_{\mathbf{n}} = \frac{1}{2}(\mathbf{I} + \lambda\sigma_{\mathbf{n}}). \quad (31)$$

Here, \mathbf{I} is the 2x2 identity matrix, the parameter $\lambda \in [-1, 1]$ gives the degree of purity of $\rho_{\mathbf{n}}$, $\text{Tr}[\rho_{\mathbf{n}}^2] = (1 + \lambda^2)/2$, and $\sigma_{\mathbf{n}}$ is the Pauli matrix corresponding to an arbitrary direction in the Bloch sphere [1], $\sigma_{\mathbf{n}} = \{\{\cos(\theta), \sin(\theta)e^{-i\phi}\}, \{\sin(\theta)e^{+i\phi}, -\cos(\theta)\}\}$, being defined by the polar angles $\theta \in [0, \pi]$ and $\phi \in [0, 2\pi]$. From Eqs. (30) and (31), the parameters of the stationary state (26) read

$$p = \frac{1}{4}[1 + \lambda_a \cos(\theta_a)][1 + \lambda_b \cos(\theta_b)], \quad (32a)$$

$$c = \frac{1}{4}\lambda_a\lambda_b \exp[-i(\phi_a + \phi_b)] \sin(\theta_a) \sin(\theta_b). \quad (32b)$$

Considering these expressions it is possible to find the set of values of $\{\lambda_a, \lambda_b, \theta_a, \theta_b, \phi_a, \phi_b\}$ that maximize the entanglement of ρ_{AB}^{∞} , that is $|c|$ [Eq. (29)]. We get $\lambda_a = \pm 1$, $\lambda_b = \pm 1$, $\theta_a = \theta_b = \pi/2$, and arbitrary values of ϕ_a and ϕ_b , delivering

$$\max_{\rho_{AB(0)}^{\text{sep}}} \{C[\rho_{AB}^{\infty}]\} = \frac{1}{2}. \quad (33)$$

Hence, over the set of all separable initial conditions, pure states lying on the $x - y$ plane lead to the maximal possible concurrence in the long time limit.

C. Evolution of entanglement and quantum-classical correlations

In Fig. 1 we plot the evolution of the concurrence taking the separable symmetric initial condition $\rho_{AB}(0) =$

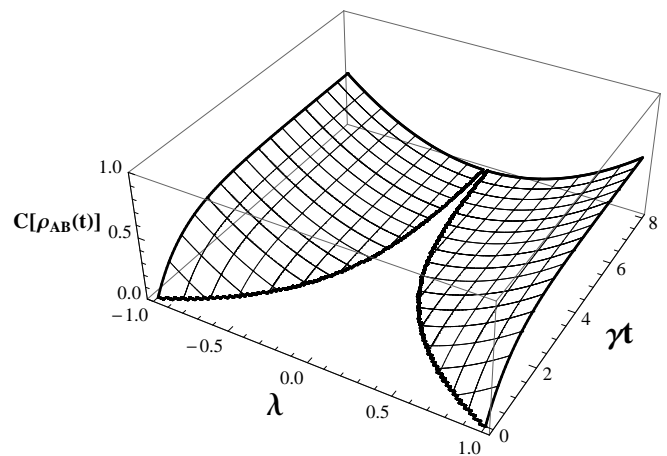


FIG. 1: Evolution of the concurrence $C[\rho_{AB}(t)]$ as a function of time for the constrained evolution defined by Eq. (25). The initial conditions are $\rho_{AB}(0) = \rho_y \otimes \rho_y$ where $\rho_y = (1/2)(\mathbf{I} + \lambda\sigma_y)$. The parameters are $\gamma_A = \gamma_B = \gamma$. The plot does not depend on the transition frequencies ω_A and ω_B .

$\rho_y \otimes \rho_y$. Each state is defined by $\rho_y = (1/2)(\mathbf{I} + \lambda\sigma_y)$, where σ_y is the y-Pauli matrix and $\lambda \in [-1, 1]$. The stationary state [Eq. (26)] becomes characterized by the coefficients $p = 1/4$ and $c = -\lambda^2/4$. From Eq. (29) the stationary concurrence reads

$$C[\rho_{AB}^{\infty}] = \frac{\lambda^2}{2}. \quad (34)$$

Consistently with the previous analysis, $C[\rho_{AB}^{\infty}] = 1/2$ only when $\lambda = \pm 1$, that is, when both systems begin in an eigenstate of σ_y . Similarly to the Dicke model [23, 36], Fig. 1 also shows that for all mixed states ($\lambda \neq \pm 1$) there exist a time delay before entanglement emerges. The birth time, τ_0 , is related to the degree of purity. When $\gamma_A = \gamma_B = \gamma$, we get

$$\gamma\tau_0 = 2 \log(1/|\lambda|). \quad (35)$$

In order to understand this result, in Fig 2(a), for $\lambda = 1/2$, we plot the four bipartite populations, while in Fig. 2(b) we plot the coherences (in a interaction representation). For the chosen initial conditions, the time evolution of the populations is the same of any value of λ . In both plots, consistently with Eq. (25), the constant matrix elements correspond to $\langle ++|\rho_{AB}(t)|++\rangle$, and $\langle ++|\rho_{AB}(t)|--\rangle$. In Fig. 2(c) we plot the concurrence and also the classical and quantum correlations (see Appendix). Comparing with the previous plot [Fig. 2(b)], it becomes evident that, for the considered initial conditions and parameters, the concurrence becomes not null when the absolute value of coherence $\langle ++|\rho_{AB}(t)|--\rangle = c$ [or equivalently $\langle --|\rho_{AB}(t)|++\rangle$] is larger than the absolute value of any other coherence. This condition, from Eq. (25), leads to the analytical result (35).

Fig. 2(c) also shows that the belated appearance of entanglement is preceded by the buildup of strong classi-

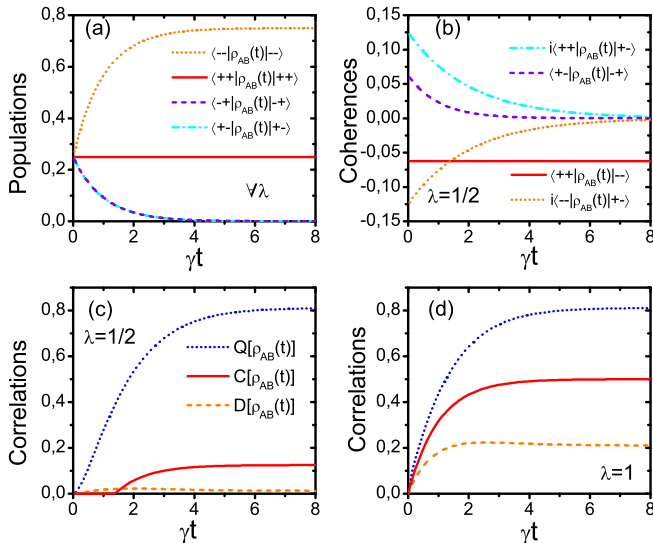


FIG. 2: Plot of matrix elements and correlations as a function of time associated to the evolution Eq. (25). The initial conditions and parameters are the same than in Fig. 1. (a) Populations, which do not depend on the value of the purity parameter λ . (b) Coherences in a representation interaction for $\lambda = 1/2$. (c) Concurrence $C[\rho_{AB}(t)]$ (full line) classical $Q[\rho_{AB}(t)]$ (dotted line) and quantum $D[\rho_{AB}(t)]$ correlations for $\lambda = 1/2$. (d) The same objects for $\lambda = 1$.

cal correlations and also moderate quantum correlations. These properties are similar to that found in Ref. [36] for an optical Dicke model. Nevertheless, here the quantum correlations have a minor weight when compared to the classical ones. On the other hand, in contrast to the Dicke model, the constrained dynamics is unable to create any entanglement when the initial condition is any of the pure separable states (24).

In Fig. 2(d) we show the time dependence of the concurrence and correlations for $\lambda = 1$, that is for a separable pure initial condition. In agreement with Eq. (35) the entanglement delay time is null. On the other hand, consistently with the previous comments, at shorter times the classical correlation growing rate is larger than the quantum one.

Most of results developed in this section also apply when the kinetic constraints (20) are defined by the projectors $\mathcal{P}_A = \mathcal{P}_B = |+\rangle\langle +|$. For example, Eq. (33) applies while Eq. (28) remains valid after the replacement $|\Phi_{\pm}\rangle \rightarrow |\Psi_{\pm}\rangle$. Similarly, with these projectors the dynamics is unable to create any entanglement if the initial conditions are the separable pure states (24).

IV. INTERPLAY BETWEEN EXTERNAL LOCAL EXCITATION AND CLASSICALLY CONSTRAINED DISSIPATION

In the previous section we showed that, even when the constraints (21) admits a classical interpretation [Eq.

(23)], the dynamics can generate some entanglement in the stationary regime. Nevertheless, the stationary concurrence depends on the initial conditions. In this section, we are interested in characterizing how these properties are affected when the systems are coupled to external local Hamiltonian fields that do not commute with the corresponding projectors. In this situation, the projector's average values can not be obtained from a classical master equation like Eq. (14). On the other hand, the external fields by they self cannot generate any entanglement. Hence, the interplay between constrained dissipation and the external excitation is the central ingredient to analyze.

A. Maximal entangled stationary state

Optical (fluorescent) two-level systems can be resonantly excited with an external laser field, such that in an interaction representation their Hamiltonian becomes $\hbar\Omega\sigma_x/2$, where the Rabi frequency Ω measures the laser strength [3]. Taking this kind of external excitation for each system, the Hamiltonian [Eq. (16)] of the optical-like qubits considered in the previous section becomes

$$H = \frac{\hbar\Omega_A}{2}\sigma_x \otimes I_B + \frac{\hbar\Omega_B}{2}I_A \otimes \sigma_x, \quad (36)$$

where σ_x is the x-Pauli matrix, Ω_A and Ω_B measure the interaction of each system with the external local fields. Eq. (36) is valid when both transition frequencies [Eq. (16)] are the same, $\omega_A = \omega_B$. At the end of this section we analyze the consequences of raising up this and other symmetry conditions. On the other hand, notice that the constraints Eq. (21) do not commute with the local Hamiltonian (36).

Trivially, the eigenvectors of H are defined by the external product of the eigenvectors of σ_x , that is $|x_{\pm}\rangle \otimes |x_{\pm}\rangle$ with eigenvalues $\pm\Omega = \pm(\Omega_A + \Omega_B)/2$, and $|x_{\pm}\rangle \otimes |x_{\mp}\rangle$ with eigenvalues $\pm\delta\Omega = \pm(\Omega_A - \Omega_B)/2$. For symmetric local excitations

$$\Omega_A = \Omega_B = \Omega, \quad (37)$$

a degeneracy arises for the null eigenvalue, $\pm\delta\Omega = 0$. It is simple to demonstrate that the Bell states $|\Phi_{-}\rangle$ and $|\Psi_{-}\rangle$ lay in the plane of degeneracy, that is, they are eigenvectors of the Hamiltonian with null eigenvalue. Taking into account the invariance defined by Eq. (28), it follows that when $\rho_{AB}(0) = |\Phi_{-}\rangle\langle\Phi_{-}|$, the dynamics defined by Eqs. (20) and (36) satisfies $\rho_{AB}(t) = \rho_{AB}(0)$. Nevertheless, for the present situation there not exist a dark state. In fact, independently of the initial condition, under the joint action of the local Hamiltonians and the constrained dissipation, the stationary state is

$$\rho_{AB}^{\infty} = \lim_{t \rightarrow \infty} \rho_{AB}(t) = |\Phi_{-}\rangle\langle\Phi_{-}|, \quad (38)$$

that is, ρ_{AB}^{∞} is a maximally entangled pure Bell state. The uniqueness of the stationary state can be proved in

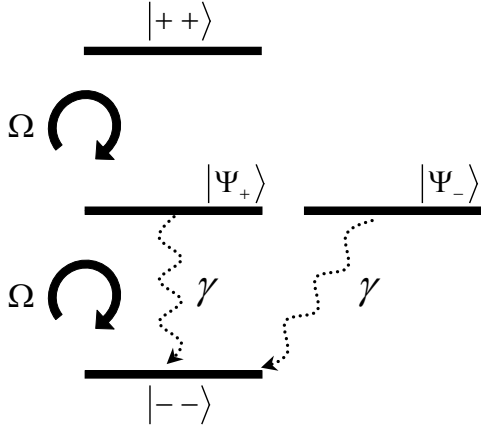


FIG. 3: Level scheme for the dynamics defined by Eqs. (15), (20), (21), and (36). The dissipative and coherent couplings are valid under the symmetry conditions $\Omega_A = \Omega_B = \Omega$, and $\gamma_A = \gamma_B = \gamma$ (see text).

a pure mathematical way (the density matrix evolution has a unique eigenoperator with null eigenvalue). Below, we understand this fact from a dynamical point of view.

B. Collective coherent-dissipative dynamics

The interplay between the unitary [Eq. (36)] and the dissipative [Eq. (25)] dynamics that leads to the stationary state (38) can be analyzed in a simpler way in the collective basis

$$|1\rangle = |++\rangle, \quad |3\rangle = |\Psi_-\rangle, \quad (39a)$$

$$|2\rangle = |\Psi_+\rangle, \quad |4\rangle = |--\rangle. \quad (39b)$$

In this basis, the Hamiltonian (36) reads

$$H = \frac{1}{\sqrt{2}} \begin{pmatrix} 0 & \Omega & \delta\Omega & 0 \\ \Omega & 0 & 0 & \Omega \\ \delta\Omega & 0 & 0 & -\delta\Omega \\ 0 & \Omega & -\delta\Omega & 0 \end{pmatrix}, \quad (40)$$

where as before $\Omega = (\Omega_A + \Omega_B)/2$, and $\delta\Omega = (\Omega_A - \Omega_B)/2$. Hence, when the condition (37) is met ($\delta\Omega = 0$), the external field only couples (coherently) the states $|++\rangle \xleftrightarrow{\Omega} |\Psi_+\rangle$ and $|\Psi_+\rangle \xleftrightarrow{\Omega} |--\rangle$.

The interplay between the coherent and dissipative dynamics can be more easily described by assuming $\gamma_A = \gamma_B = \gamma$. While this is not a necessary condition for the validity of Eq. (38), under that condition the dissipative dynamics written in the collective basis (39) can be read from Eq. (25) under the replacements $\gamma_A \rightarrow \gamma$, $\gamma_B \rightarrow \gamma$. In Fig. 3 we show the levels scheme as well as the dissipative and coherent coupling valid for $\gamma_A = \gamma_B = \gamma$ and $\Omega_A = \Omega_B = \Omega$. The state $|\Psi_-\rangle$ is not affected by the unitary dynamic and it can only decay to the state $|--\rangle$. Thus, the dynamics can be reduced to the remaining three collective states. The dynamics of the states

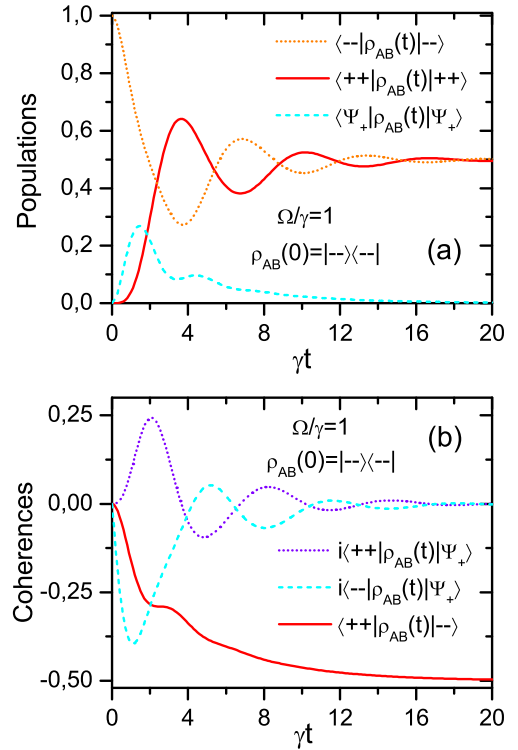


FIG. 4: (a) Collective populations as function of time. (b) Evolution of collective coherences. These plots correspond to the dynamics (15) with the Hamiltonian Eq. (36) and the constraints defined by Eqs. (20) and (21). The initial condition is $\rho_{AB}(0) = |--\rangle \langle --|$. The parameters are $\Omega_A = \Omega_B = \Omega$ and $\gamma_A = \gamma_B = \gamma$, with $\Omega/\gamma = 1$.

$|\Psi_+\rangle$ and $|--\rangle$ is equivalent to a fluorescent system [3] with Rabi frequency Ω and natural decay γ . The role of upper and lower states is played by $|\Psi_+\rangle$ and $|--\rangle$ respectively. As a consequence of the constraints, the state $|++\rangle$ does not decay. Nevertheless, it is coupled coherently to the state $|\Psi_+\rangle$. $|++\rangle$ and $|\Psi_+\rangle$ play the role of upper and lower levels respectively.

The opposite roles played by $|\Psi_+\rangle$, jointly with uncoupling of the state $|++\rangle$ from the reservoir decay dynamics leads to (i) an asymptotic depopulation of the state $|\Psi_+\rangle$, (ii) a raising of the $|++\rangle \leftrightarrow |--\rangle$ coherence, and (iii) an asymptotic vanishing of the difference of the $|++\rangle$ and $|--\rangle$ occupations (populations). This coherent-dissipative mechanism drives the system to the Bell state $|\Phi_-\rangle$ independently of the initial condition, Eq. (38).

In order to clarify the previous mechanism, in Fig. 4 we plot the time dependence of the collective populations and coherences. The density matrix evolution (15) is defined by the Hamiltonian Eq. (36) and the constraints introduced in Eqs. (20) and (21). The parameters are $\Omega_A = \Omega_B = \Omega$ and $\gamma_A = \gamma_B = \gamma$, with $\Omega/\gamma = 1$. At the initial time both systems are in their respective lower states, $\rho_{AB}(0) = |--\rangle \langle --|$. Notice that without the external fields the systems remain at all times in this state.

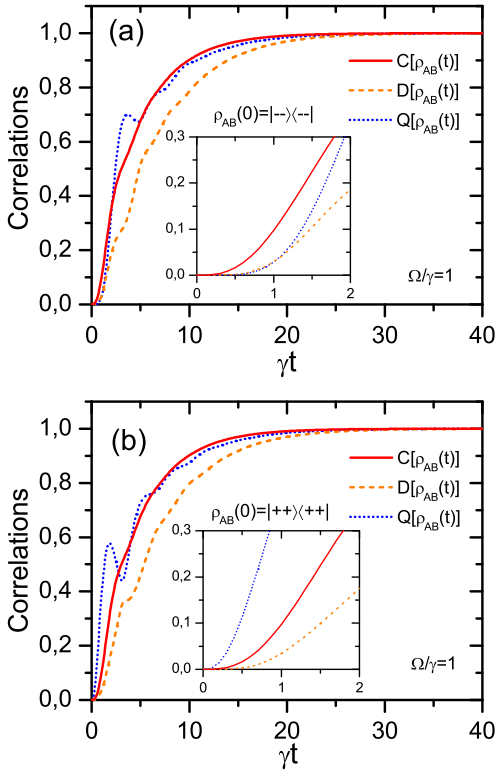


FIG. 5: Plot of Concurrence $C[\rho_{AB}(t)]$ (full line) classical $Q[\rho_{AB}(t)]$ (dotted line) and quantum $D[\rho_{AB}(t)]$ (dashed line) correlations. The parameters and evolution of $\rho_{AB}(t)$ are the same than in Fig. 4. (a) Time dependence corresponding to the initial condition $\rho_{AB}(0) = |--\rangle\langle--|$. (b) Initial condition $\rho_{AB}(0) = ++\rangle\langle++|$. In both insets we show the short time behavior of the correlations.

Furthermore, with this initial condition and parameters the state $|\Psi_{-}\rangle$ is never populated.

Fig. 4(a) shows the dissipative-coherent interplay that lead to a vanishing of the $|\Psi_{+}\rangle$ population. Furthermore, as expected the population of states $|++\rangle$ and $|--\rangle$ oscillates with opposite phases, while in the long time regime both of them become equal to one half. In Fig. 4(b), we show the collective coherences. Coherences involving the state $|\Psi_{+}\rangle$ vanish asymptotically, while the coherence between the states $|++\rangle \leftrightarrow |--\rangle$ converges to minus one half. The asymptotic value of the coherence $\langle ++|\rho_{AB}(t)|--\rangle$ and the populations $\langle ++|\rho_{AB}(t)|++\rangle$, $\langle --|\rho_{AB}(t)|--\rangle$, indicate that the bipartite dynamics achieve the pure Bell state $|\Phi_{-}\rangle$.

In Fig. 5(a), we show the time evolution of concurrence and the classical-quantum correlations corresponding to the dynamic shown in Fig. 4, that is, for the initial condition $\rho_{AB}(0) = |--\rangle\langle--|$. As the dynamics in the long time regime reaches a maximal entangled state, all correlations converge to one. On the other hand, the short time behavior strongly departs from that shown in Fig. 2(d). In fact, here the concurrence $C[\rho_{AB}(t)]$ grows much faster than the classical and quantum contributions, $Q[\rho_{AB}(t)]$ and $D[\rho_{AB}(t)]$. In contrast, in Fig

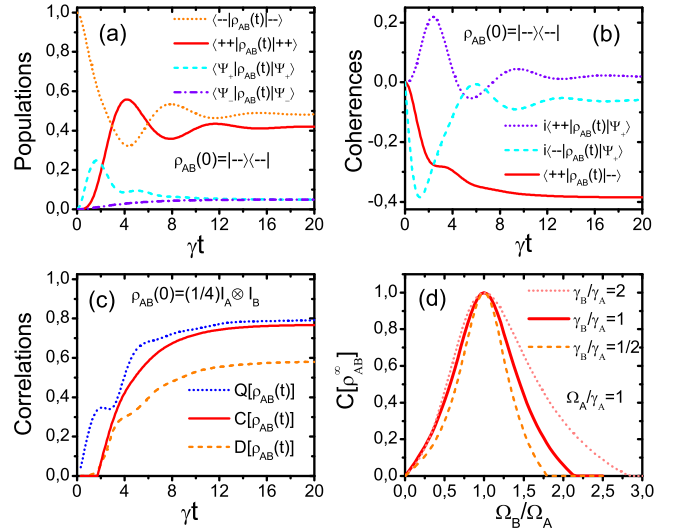


FIG. 6: (a) Collective populations as function of time. (b) Evolution of collective coherences. (c) Concurrence and classical-quantum correlations. (d) Stationary concurrence as a function of Ω_B/Ω_A for different values of γ_B/γ_A . All these plots correspond to the dynamics (15) with the Hamiltonian Eq. (36) and the constraints defined by Eqs. (20) and (21). In plots (a), (b), and (c) the parameters are $\gamma_A = \gamma_B = \gamma$, $\Omega_A/\gamma = 1$, and $\Omega_B/\gamma = 3/4$. The initials conditions are indicated in each plot.

5(b) a similar behavior to that shown in Fig. 2(d) is recovered. The initial condition is $\rho_{AB}(0) = ++\rangle\langle++|$. These results demonstrate that at short times the relative weights of each correlation have a strong dependence on the dynamics and initial conditions under consideration.

C. Breaking symmetries conditions

While we have considered the projectors defined by Eq. (20) and (21), the same result can be achieved with $\mathcal{P}_A = \mathcal{P}_B = |+\rangle\langle+|$. In this case, the pure stationary state is $|\Psi_{+}\rangle$. On the other hand, the achievement of a maximal entangled state relies on the validity of some symmetry assumptions. Below, we analyze what happens when they are not meet.

For the dynamics defined by projectors (21), the assumption $\omega_A = \omega_B$ can be raised up. In fact, by denoting the frequency of the external (laser) excitation by ω_L , instead of the resonant condition $\omega_L = \omega_A = \omega_B$, for $\omega_A \neq \omega_B$ one must to choose $\omega_L = (\omega_A + \omega_B)/2$. Thus, in an interaction representation with respect to $\hbar\omega_L[\sigma_z \otimes I_B + I_A \otimes \sigma_z]/2$, the Hamiltonian (36) acquires the extra contribution $\hbar(\omega_A - \omega_B)[\sigma_z \otimes I_B - I_A \otimes \sigma_z]/2$. Under the condition $\Omega_A = \Omega_B$ the same maximal entangled state is obtained.

In Fig. 6 we analyze the stationary entanglement when the Rabi frequencies are different. We conclude that the previous results are not a singular property that only

happens when $\Omega_A = \Omega_B$, that is, for $|\Omega_A - \Omega_B| \ll (\Omega_A + \Omega_B)$ it follows $C[\rho_{AB}^\infty] \simeq 1$.

In Fig. 6(a) we show the collective populations. In comparison with Fig. 4(a) (same initials conditions, $\rho_{AB}(0) = |--\rangle\langle--|$), here the population $\langle\Psi_-|\rho_{AB}(t)|\Psi_- \rangle$ becomes populated in the stationary regime, indicating the departure of ρ_{AB}^∞ from a maximal entangled state. This fact is corroborated in Fig. 6(b), where $|\langle++|\rho_{AB}^\infty|--\rangle| < 1/2$. Furthermore, (not shown) coherences involving the state $|\Psi_- \rangle$ also become not null. These departures arise because the condition $\Omega_A \neq \Omega_B$ eliminate the eigenvectors degeneracy of the unitary dynamics [see Eq. (40)].

In Fig. 6(c) we plot the evolution of the concurrence and the classical-quantum correlations. The initial condition is the identity matrix, $\rho_{AB}(0) = (\mathbf{I}_A \otimes \mathbf{I}_B)/4$. As expected, the concurrence does not converge to one. On the other hand, for this initial condition a delayed birth of entanglement is observed. As in previous section, it is preceded by a fast increasing of the classical correlation and a very small contribution of the quantum correlation.

In Fig. 6(d) we plot the stationary concurrence, $C[\rho_{AB}^\infty]$, as a function of Ω_B/Ω_A for different values of γ_B/γ_A . Independently of this last parameter, for $\Omega_B/\Omega_A = 1$ we get $C[\rho_{AB}^\infty] = 1$. On the other hand, high concurrence values can be achieved around this point. These curves demonstrate the robustness of the dynamics for generating almost pure entangled states even when the symmetry conditions are not meet exactly. In order to quantify this property, we calculated the stationary density matrix for $\gamma_A = \gamma_B = \gamma$ and $\Omega_B \neq \Omega_A$. To first order in $\delta\Omega = (\Omega_A - \Omega_B)/2$, in the product basis Eq. (24), we get

$$\rho_{AB}^\infty = \begin{pmatrix} \frac{1}{2} & -i\frac{\delta\Omega}{\gamma} & i\frac{\delta\Omega}{\gamma} & -\frac{1}{2} \\ i\frac{\delta\Omega}{\gamma} & 0 & 0 & -i\frac{\delta\Omega}{\gamma} \\ -i\frac{\delta\Omega}{\gamma} & 0 & 0 & i\frac{\delta\Omega}{\gamma} \\ -\frac{1}{2} & i\frac{\delta\Omega}{\gamma} & -i\frac{\delta\Omega}{\gamma} & \frac{1}{2} \end{pmatrix} + O(\delta\Omega^2). \quad (41)$$

On the other hand, from the exact expression for ρ_{AB}^∞ , the stationary concurrence can be written as

$$C[\rho_{AB}^\infty] = 1 - \left(\frac{16}{\gamma^2} + \frac{2}{\Omega^2} \right) \delta\Omega^2 + O[\delta\Omega^3], \quad (42)$$

where $\Omega = (\Omega_A + \Omega_B)/2$. Therefore, the concurrence decreases in a quadratic way with the asymmetry $\delta\Omega$.

V. SUMMARY AND CONCLUSIONS

We characterized a class of constrained quantum dissipative evolution where dynamical constraints are introduced through a set of projectors that conditioning the action of each dissipative (Lindblad) channel to the state of the other system, Eqs. (1) and (4). When the set of projectors is closed under the dynamical action of each dissipative dynamic, Eq. (10), the kinetic constraints can

be read in a classical way, that is, the reduced density matrixes evolve with a Lindblad rate equation, Eq. (11), and the conditional expectation values of the projectors are defined by a classical master equation, Eq. (14).

With the previous ingredients, we studied the stationary entanglement that can be achieved by two optical-like qubits whose individual decay dynamics is only possible when the other system is in the lower state. This classical constraint lead to a free decoherence state, which play a central role in the entanglement generation. Under the solely action of the dissipative dynamics, the stationary entanglement depends on the initial condition. Maximal entangled states are unreachable from separable initial states. On the contrary, we showed that by coupling the systems to local external Hamiltonian fields, Eq. (36), the interplay between the coherent and dissipative effects drive the systems to a maximal entangled Bell state, Eq. (38). This property does not depends on the system initialization. The coherent dynamic that couple the free decoherence state (induced by the constraints) and its complementary space is the central ingredient that give rise to this property. The underlying mechanism can be understood in a collective basis, where a Bell state play the role of lower an upper level for the coherent and incoherent couplings induced by the external excitation and the constrained dynamics respectively (Fig. 3).

We also studied the time evolution of the entanglement. The present model confirm that quantum and classical correlations between the systems are precursors of the entanglement, that is, the arise before entanglement emerges. Nevertheless, in contrast to other dynamics such as the Dicke model [36], here the weights of both correlations may strongly depend on both the initial conditions and the external excitation.

Our analyses applies to bipartite systems. Due to the present advances in engineered system-bath coupling constrained dynamics could be checked in that context. On the other hand, the present results may apply when restricting the dynamics of a complex many body system to a given bipartite subspace.

Acknowledgments

This work was supported by Consejo Nacional de Investigaciones Científicas y Técnicas (CONICET), Argentina, under Grant No. PIP 11420090100211.

Appendix: Entanglement measure and quantum-classical correlations

Here, we provide the definition of the correlation measures used along the manuscript. The entanglement measure associated to the entanglement of formation [4] is the concurrence. For a bipartite state ρ_{AB} it is defined as

$$C[\rho_{AB}] = \max\{0, \sqrt{\lambda_1} - \sqrt{\lambda_2} - \sqrt{\lambda_3} - \sqrt{\lambda_4}\}. \quad (A.1)$$

$\{\lambda_i\}_{i=1}^{i=4}$ are the eigenvalues (written in decreasing order) of the matrix $\rho_{AB}\tilde{\rho}_{AB}$, where $\tilde{\rho}_{AB} = \sigma_x \otimes \sigma_x \rho_{AB}^* \sigma_x \otimes \sigma_x$, and ρ_{AB}^* is the conjugate of ρ_{AB} in the computational basis. For the stationary state (26), the eigenvalues $\{\lambda_i\}_{i=1}^{i=4}$ are $\{(\sqrt{p(1-p)} \pm |c|)^2, 0, 0\}$, which leads to Eq. (29).

The mutual information provides a measure of the total correlations in a bipartite setup

$$\mathcal{I}(\rho_{AB}) = S(\rho_A) + S(\rho_B) - S(\rho_{AB}), \quad (\text{A.2})$$

where the Shannon entropy reads $S(\rho) = -\text{Tr}\{\rho \log_2 \rho\}$, and $\rho_A = \text{Tr}_B[\rho_{AB}]$, $\rho_B = \text{Tr}_A[\rho_{AB}]$. $\mathcal{I}(\rho_{AB})$ can be written as the addition of a classical contribution [7], $\mathcal{Q}(\rho_{AB})$, and a quantum contribution or discord [8], $\mathcal{D}(\rho_{AB})$,

$$\mathcal{I}(\rho_{AB}) = \mathcal{Q}(\rho_{AB}) + \mathcal{D}(\rho_{AB}). \quad (\text{A.3})$$

The classical correlation is defined as

$$\mathcal{Q}(\rho_{AB}) = \sup_{\{\Pi_{\mathbf{n}}\}} \{S(\rho_A) - S(\rho_{AB}|\Pi_{\mathbf{n}})\}, \quad (\text{A.4})$$

while the discord reads

$$\mathcal{D}(\rho_{AB}) = \inf_{\{\Pi_{\mathbf{n}}\}} \{\mathcal{I}(\rho_{AB}) - S(\rho_{AB}|\Pi_{\mathbf{n}})\}. \quad (\text{A.5})$$

In both expressions, $S(\rho_{AB}|\Pi_{\mathbf{n}})$ refers to the conditional entropy of system A given that a measurement over system B was performed. This action can be defined by a measurement in an arbitrary direction \mathbf{n} over the Bloch sphere. Thus, $\{\Pi_{\mathbf{n}}\} = \Pi_{\mathbf{n}\pm}(\theta, \phi) = |\mathbf{n}_{\pm}\rangle\langle\mathbf{n}_{\pm}|$, where

$$|\mathbf{n}_+\rangle = +\cos(\theta/2)|+\rangle + e^{+i\phi}\sin(\theta/2)|-\rangle, \quad (\text{A.6a})$$

$$|\mathbf{n}_-\rangle = -\sin(\theta/2)|+\rangle + e^{i\phi}\cos(\theta/2)|-\rangle. \quad (\text{A.6b})$$

In this way, the extremization of Eqs. (A.4) and (A.5) is performed over the polar angles θ and ϕ .

For the stationary state ρ_{AB}^∞ , Eq. (26), it is simple to realize that it is always possible to chose a projector

$\Pi_{\mathbf{n}}$ ($\theta = 0, \pi, \pi/2$) such that the minimal value of the conditional entropy $S(\rho_{AB}|\Pi_{\mathbf{n}})$ is zero. Hence, it follows

$$\mathcal{Q}(\rho_{AB}^\infty) = S(\rho_A^\infty) = S(\rho_B^\infty), \quad (\text{A.7})$$

while the stationary discord becomes

$$\mathcal{D}(\rho_{AB}^\infty) = S(\rho_A^\infty) - S(\rho_{AB}^\infty) = S(\rho_B^\infty) - S(\rho_{AB}^\infty). \quad (\text{A.8})$$

The entropies $S(\rho) = -\text{Tr}\{\rho \log_2 \rho\}$ can trivially be determine from the eigenvalues of the corresponding matrixes. The four eigenvalues of ρ_{AB}^∞ are $\{\frac{1}{2}[1 \pm \sqrt{1 - 4p(1-p) + 4|c|^2}], 0, 0\}$. From here, one deduce that the stationary discord $\mathcal{D}(\rho_{AB}^\infty)$ is not null only when $|c| \neq 0$, that is, the same condition for getting a non null stationary concurrence, Eq. (29).

The initial conditions and dynamics considered along the paper lead to a bipartite density matrix ρ_{AB} with the structure

$$\rho_{AB} = \begin{pmatrix} q & -id & -id' & w \\ id & r & u & -iv \\ id' & u & r' & -iv' \\ w & iv & iv' & s \end{pmatrix}, \quad (\text{A.9})$$

where each letter represent a real number. For symmetric states, $\rho_A = \rho_B$, it follows $d' = d$, $v' = v$, $r' = r$. The concurrence of this kind of state can be calculated in an analytical way. Nevertheless, the expression becomes very complicated and does not provide useful information. On the other hand, we find that $S(\rho_{AB}|\Pi_{\mathbf{n}})$ is minimal (with the same value) at angles $\phi = \pi/2$ and $\phi = 3\pi/2$. Nevertheless, consistently with the analysis of Ref. [41] the value of θ must to be found in a numerical way. When ρ_{AB} adopts a X structure, $\{d = d' = v = v' = 0\}$, the implemented numerical algorithm recovers the analytical discord values presented in Ref. [42].

-
- [1] M.A. Nielsen and I.L. Chuang, *Quantum Computation and Quantum Information*, (Cambridge University Press, Cambridge, 2000).
- [2] R. Horodecki, P. Horodecki, M. Horodecki, and K. Horodecki, *Rev. Mod. Phys.* **81**, 865 (2009).
- [3] H.P. Breuer and F. Petruccione, *The theory of open quantum systems*, Oxford University press (2002).
- [4] W.K. Wootters, *Phys. Rev. Lett.* **80**, 2245 (1998).
- [5] T. Yu and J.H. Eberly, *Phys. Rev. Lett.* **93**, 140404 (2004).
- [6] Z. Ficek, and R. Tanas, *Phys. Rev. A* **74**, 024304 (2006).
- [7] L. Henderson and V. Vedral, *J. Phys. A* **34**, 6899 (2001).
- [8] H. Ollivier and W.H. Zurek, *Phys. Rev. Lett.* **88**, 017901 (2001).
- [9] J. Maziero, L.C. Celeri, R.M. Serra, and V. Vedral, *Phys. Rev. A* **80**, 044102 (2009).
- [10] L. Mazzola, J. Piilo, and S. Maniscalco, *Phys. Rev. Lett.* **104**, 200401 (2010).
- [11] F. Benatti, R. Floreanini, and M. Piani, *Phys. Rev. Lett.* **91**, 070402 (2003).
- [12] L. Jakóbczyk, *J. Phys. A* **35**, 6383 (2002).
- [13] K. Lendi and A.J. van Wonderen, *J. Phys. A* **40**, 279 (2007).
- [14] B. Baumgartner, H. Narnhofer, and W. Thirring, *J. Phys. A* **41**, 065201 (2008).
- [15] M.S. Kim, J. Lee, D. Ahn, and P.L. Knight, *Phys. Rev. A* **65**, 040101(R) (2002).
- [16] D. Braun, *Phys. Rev. Lett.* **89**, 277901 (2002).
- [17] J.-H. An, S.-J. Wang, and H.-G. Luo, *J. Phys. A* **38**, 3579 (2005).
- [18] M. Hor-Meyll, A. Auyuanet, C.V.S. Borges, A. Aragao, J.A.O. Huguenin, A.Z. Khoury, and L. Davidovich, *Phys. Rev. A* **80**, 042327 (2009).
- [19] L. Derkacz and L. Jakóbczyk, *J. Phys. A* **41**, 205304 (2008).
- [20] F. Benatti, R. Floreanini, and U. Marzolino, *Phys. Rev.*

- A **81**, 012105 (2010).
- [21] L. Jakóbczyk and A. Jamróz, *Phys. Lett. A* **318**, 318 (2003).
- [22] R. Tanas and Z. Ficek, *J. Opt. B: Quantum Semiclass. Opt.* **6**, S90 (2004).
- [23] Z. Ficek, and R. Tanas, *Phys. Rev. A* **77**, 054301 (2008); A.F. Alharbi and Z. Ficek, *Phys. Rev. A* **82**, 054103 (2010).
- [24] Q.F. Xu, X.Z. Hui, J.N. Chen, and Z. Cheng, *Eur. Phys. J. D* **66**, 86 (2012).
- [25] A.-S.F. Obada, S.A. Hanoura, and A.A. Eied, *Eur. Phys. J. D* **66**, 221 (2012).
- [26] J. Roden, A. Eisfeld, W. Wolff, and W.T. Strunz, *Phys. Rev. Lett* **103**, 058301 (2009).
- [27] A. Thilagam, *J. Phys. A* **44**, 135306 (2011).
- [28] G.H. Fredrickson and H.C. Andersen, *Phys. Rev. Lett.* **53**, 1244 (1984); *J. Chem. Phys.* **83**, 5822 (1985); R.G. Palmer, D.L. Stein, E. Abrahams, and P.W. Anderson, *Phys. Rev. Lett.* **53**, 958 (1984).
- [29] M.A. Muñoz, A. Gabrielli, H. Inaoka, and L. Pietronero, *Phys. Rev. E* **57**, 4354 (1998).
- [30] J.P. Garrahan and D. Chandler, *Phys. Rev. Lett.* **89**, 035704 (2002).
- [31] D. Chandler and J.P. Garrahan, *Annu. Rev. Phys. Chem.* **61**, 191 (2010).
- [32] F. Ritort and P. Sollich, *Advances in Physics* **52**, 219 (2003).
- [33] B. Olmos, I. Lesanovsky, and J.P. Garrahan, *Phys. Rev. Lett.* **109**, 020403 (2012).
- [34] A.A. Budini, *Phys. Rev. A* **74**, 053815 (2006); *Phys. Rev. E* **72**, 056106 (2005); H.P. Breuer, *Phys. Rev. A* **75**, 022103 (2007).
- [35] A.A. Budini, *Phys. Rev. A* **79**, 043804 (2009); *J. Phys. B: At. Mol. Phys.* **43**, 115501 (2010).
- [36] A. Auyuanet and L. Davidovich, *Phys. Rev. A* **82**, 032112 (2010).
- [37] M.A. Gallego, R. Coto, and M. Orszag, *Phys. Scr.* **T147**, 014012 (2012).
- [38] Y.Q. Zhang and J.B. Xu, *Eur. Phys. J. D* **64**, 549 (2011).
- [39] J.S. Zhang, L. Chen, M. Abdel-Aty, and A.X. Chen, *Eur. Phys. J. D* **66**, 2 (2012).
- [40] T. Wu and L. Ye, *Eur. Phys. J. D* **66**, 261 (2012).
- [41] D. Girolami and G. Adesso, *Phys. Rev. A* **83**, 052108 (2011).
- [42] F.F. Fanchini, T. Werlang, C.A. Brasil, L.G.E. Arruda, and A.O. Caldeira, *Phys. Rev. A* **81**, 052107 (2010); M. Ali, A.R.P. Rau, and G. Alber, *Phys. Rev. A* **81**, 042105 (2010); S. Luo, *Phys. Rev. A* **77**, 042303 (2008).